Study of Filled SBR Elastomers Using NMR and Mechanical Measurements

Huijun Luo,[†] Manfred Klüppel,[‡] and Horst Schneider*,[†]

Fachbereich Physik, Martin-Luther-Universität Halle-Wittenberg, Friedemann-Bach-Platz 6, D-06108 Halle/Saale, Germany, and Deutsches Institut für Kautschuktechnologie e. V., Eupener Str. 33, D-30519 Hannover, Germany

Received December 23, 2003; Revised Manuscript Received June 15, 2004

ABSTRACT: The effects of different kinds and amounts of fillers, e.g., carbon black N220 and silica−silane, on molecular structure and dynamics of styrene−butadiene rubber (SBR) and the effects of vulcanization on filled SBR systems are studied by Hahn echo and rotating-frame longitudinal relaxation $T_{1\rho}$ NMR techniques as well as mechanical measurements, with the emphasis of quantitative comparison between microscopic and macroscopic results. The calculation based on a theoretic model for transverse relaxation in elastomeric networks reveals that filler aggregates or clusters behave like additional cross-linking points and thus lead to a decrease in the molecular mass between cross-linking points M_c, an increase of intercross-link chains, or accordingly a decrease of dangling and free chains, ultimately to the increasing cross-link modulus G_c, to the extent that depends on the type and, in particular, content of fillers. Compared with SBR filled with silica−silane, SBR filled with carbon black N220 shows more network chains due to its stronger binding ability or adsorbability but results in less cross-link density due to its higher inhomogeneity. The filler dependence of segmental and overall chain mobility is definitely different for both SBR systems, cross-linked and un-cross-linked, which is attributed to the restriction of filler on chemical cross-linking reaction occurred in a SBR matrix. A recent concept of hydrodynamic reinforcement by filler clusters and stress-induced cluster breakdown is combined with a tube model of rubber elasticity for modeling the typical stress softening effect of filled rubber for uniaxial stress−strain measurements. The evaluated material parameters deliver information about cross-link densities and filler specific polymer−filler couplings. The resulting densities ν_{mech} of network junctions are fairly consistent with NMR-derived ones within experimental errors; the differences can be used to estimate the content of different types of cross-links and chain entanglements. Finally, the related observations have been schematically represented using different physical models.

Introduction

It is well-known that the incorporation of nanoscopic fillers as carbon black, silica, or polymeric microgels in an elastomer can markedly improve the mechanical, electrical, and other properties of elastomeric polymers. The effect of fillers on reinforcement of a rubber is of scientific and commercial importance. A great amount of effort and many detection techniques, e.g., TEM, DSC, SAXS, swelling and mechanical measurements, neutron scattering technique, pulsed NMR spectroscopy, and so forth, have been dedicated to understand the effect of fillers on the rubber matrix. Among them, solid-state NMR techniques, including fast-speed MAS or CP/MAS, spin echo and $T_{1\rho}$, line width measurements, etc., are powerful tools of directly probing structural and dynamic information about filled elastomers on a molecular level. In our previous papers it has been already shown that Hahn echo is a fast and advantageous technique in characterizing structural and dynamic behavior of elastomers.[1−3] Usually, for such elastomeric networks as natural rubber (NR), polybutadiene (PB), poly(dimethylsiloxane) (PDMS), and styrene−butadiene rubber (SBR), the typical transverse magnetization decay (TMD) is characteristic of both solidlike and liquidlike behavior at temperatures above $T_g + 120$ K. On the basis of these motional characteristics as revealed by TMD and on the theoretical model we proposed previously,[1−3] network structure parameters, e.g., the average molar mass between two cross-links M_c, can then be determined. We have successfully studied cross-linked elastomeric systems with emphasis on the effect of chemical cross-linking and mainly concluded that the amount of inter-cross-link chains increases, and thus the corresponding M_c decreases with increasing the cross-linker, concomitant with the lowering of segmental and overall chain mobility.[1−3] The resulting cross-link density is fairly consistent with that from mechanical measurements.[1] However, for filled elastomers the effects of filler type and amount were not systematically studied in our previous work as yet.

In this work we extend the application of the related theoretical model to filled elastomers and more systematically examine the influence of different types and amount of fillers on the rubber matrix, whether un-cross-linked or cross-linked, mainly using NMR techniques, including Hahn echo and $T_{1\rho}$. To explain, on a molecular level, different effects of both kinds of fillers, carbon black and silica−silane, two structural representations of a rubber−filler mix are schematically proposed here. On the other hand, stress−strain measurements are performed on the same samples and, on a macroscopic level, reveal the additional effect of fillers. To explain the observed stress−strain relationship, a non-Gaussian tube model with nonaffine tube deforma-

[†] Martin-Luther-Universität Halle-Wittenberg.
[‡] Deutsches Institut für Kautschuktechnologie e. V.
* Corresponding author: e-mail schneider@physik.uni-halle.de.

10.1021/ma035985u CCC: $27.50
Published on Web 09/23/2004

tions, which has been successfully applied to unfilled elastomers,[1,4,5] was extended to filled systems by including hydrodynamic reinforcement and stress-softening effects of the fillers.[6] Then from stress−strain data the cross-link density ν_{mech} was calculated and compared with the values obtained from NMR analysis.

Theoretical Section

NMR Analysis of Elastomers. In the single-pulse measurements, the magnetic susceptibility effect of fillers can influence TMD and thus complicate the explanation of the transverse relaxation behavior of elastomers. Therefore, here the Hahn echo technique was utilized to refocus the effect of filler susceptibility and detect TMD of all the SBR samples. TMD obtained in this way is only involved in segmental/chain mobility and structural features of elastomers. Usually the transverse magnetization decay of elastomers well above T_g can be formulated by the following theoretic expression that is extended on a basis of single-chain model and tube model:[7−9]

$$M_t/M_0 = A\exp\{-t/T_2 - qM_2\tau_s^2[\exp(-t/\tau_s) + t/\tau_s - 1]\} + B\exp(-t/T_2) + C\exp(-T_{2s}) \quad (1)$$

Here, A, B, and C are the relative parts of protons in inter-cross-link chains, dangling chain ends, and sol fraction in the system, respectively, T_2 is the transversal relaxation time related to the fast segmental motion, τ_s is the correlation time for overall chain motion, T_{2s} is the transversal relaxation time of "sol" fraction, and qM_2 is the mean residual part of the second moment of the dipolar interaction. In this model, the local motion of inter-cross-link chains is considered as anisotropic due to physical and chemical constraints, e.g., entanglements and cross-linking, so that dipolar interaction between a nuclear spin pair cannot be completely averaged out. On the other hand, it will be further reduced by overall chain motion, i.e., large-scale rearrangements. Hence, inter-cross-link chains usually result in a Gaussian-like contribution to the initial part of TMD. In contrast, dangling and free (or sol) chains hardly or little suffer from the motional constraints. So their motion is assumed to be isotropic (liquidlike), and the corresponding TMD will possess pure exponential feature. On the basis of eq 1, the fractions of inter-cross-link, dangling, and free chains and their corresponding mobility can be accurately determined. The relationship between the correlation time τ_f and T_2 for local segmental motion conforms to[10]

$$T_2^{-1} = M_2\tau_f\left(1 + \frac{5/3}{1+\omega_0^2\tau_f^2} + \frac{2/3}{1+4\omega_0^2\tau_f^2}\right) \quad (2)$$

Furthermore, in terms of Gotlib's idea of the factor q as the ratio between the second moments well above the glass transition temperature T_g and that of the rigid lattice (or the part of the residual dipolar interaction after averaging by a fast, anisotropic motion), the average molecular weight of inter-cross-link chains M_c can be estimated.[11] The molar mass M_c between two junction points (cross-links, entanglements, or filler junctions) can be calculated from the molar mass of a statistical segment M_{ss} and the number of these segments between two junction points N using the relation

$$q = \frac{M_2^R}{M_2} = \left(\frac{3k}{5N}\right)^2 \quad (3a)$$

$$M_c = NM_{ss} = \frac{3k}{5}\frac{M_{ss}}{\sqrt{q}} \quad (3b)$$

k is a factor which, as suggested by Fry,[12] takes into consideration the averaging over the orientations of all inter-spin vectors relative to the segmental axis. The value of k was calculated for SBR and is about 0.466 on the assumption of the rigid rod of a segment. For SBR the second moment of the rigid lattice has the value $M_2 = 0.95 \times 10^4$ ms^{-2}, and $M_{ss} = 211$ g/mol can be obtained from literature data[13,14] by applying a weight-average mixing rule. For ν_{NMR}, the number of elastically active network chains per unit volume of the rubber matrix (corrected for the dangling ends and the sol fraction), it holds

$$\nu_{NMR} = A\rho/M_c \quad (4)$$

with the mass density of SBR $\rho = 0.9$ g/cm^3 and A according to eq 1.

To separate the M_c values of network chains emanating from the entanglements and such ones associated with chemical cross-links, one has simply to build the reciprocal difference of M_c^{tot} for a cross-linked sample (with q) and un-cross-linked USBR (with q_0); i.e., $\sqrt{q}$ in the denominator of eq 3a must be replaced by $(\sqrt{q} - \sqrt{q_0})$ (in the following designated as "q_0 correction", leading to the value M_c^{cor}). In an analogous manner the chain densities associated with the polymer/filler junctions can be separated using the difference of the network densities for filled and unfilled samples (with and without cross-linking).

Both separation procedures are, of course, rough estimations only because of the assumptions that in the first case the number of entanglements during the vulcanization process is constant and in the second case the number of cross-links and entanglements does not change under the presence of filler (see discussion below).

Stress−Strain Analysis of Filler Reinforced Elastomers. For the description of rubber elasticity we use an extended, non-Gaussian, nonaffine tube model with tube deformation law $d_\mu = d_0\lambda_\mu^{1/2}$. This leads to the following elastic strain energy density W, as more closely considered in refs 1, 6, and 15:

$$W = \frac{G_c}{2}\left\{\frac{(\sum_{\mu=1}^{3}\lambda_\mu^2 - 3)\left(1 - \frac{T_e}{n_e}\right)}{1 - \frac{T_e}{n_e}(\sum_{\mu=1}^{3}\lambda_\mu^2 - 3)} + \ln\left[1 - \frac{T_e}{n_e}(\sum_{\mu=1}^{3}\lambda_\mu^2 - 3)\right]\right\} + 2G_e(\sum_{\mu=1}^{3}\lambda_\mu^{-1} - 3) \quad (5)$$

Here, λ_μ is the internal strain ratio of the polymer network, G_c is the cross-link modulus (proportional to the density of chemical cross-links), G_e is the topological

constraint modulus (proportional to the density of entanglements of the rubber), n_e is the number of chain segments between two entanglements, and T_e is the trapping factor of entanglements ($0 < T_e < 1$).

In the case of uniaxial extensions with $\lambda_1 = \lambda$, $\lambda_2 = \lambda_3 = \lambda^{-1/2}$ this yields for the apparent stress $\sigma_{0,\mu} = \partial W/\partial\lambda\mu$:

$$\sigma_{0,1} = G_c(\lambda - \lambda^{-2}) \frac{1 - \frac{2T_e}{n_e} + \left(\frac{T_e}{n_e}\right)^2\left(\lambda^2 + \frac{2}{\lambda} - 3\right)}{\left[1 - \frac{T_e}{n_e}\left(\lambda^2 + \frac{2}{\lambda} - 3\right)\right]^2} + 2G_e(\lambda^{-1/2} - \lambda^{-2}) \quad (6)$$

This equation applies to the case of unfilled polymer networks. The presence of filler clusters in filler-reinforced polymer networks leads to additional effects. Based on the concept developed in ref 6, a constitutive model of stress softening is applied that considers hydrodynamic reinforcement by filler clusters together with stress-induced filler cluster breakdown. Hydrodynamic reinforcement refers to a strain amplification factor X that relates the internal strain ratio λ_μ of the rubber matrix to the external strain ϵ_μ of the sample:

$$\lambda_\mu := 1 + X\epsilon_\mu \quad (7)$$

For the first stretching of a virgin sample the strain amplification factor X does not remain constant but is a function of external strain, i.e., $X = X(\epsilon_\mu)$. It will start at some maximum and will diminish with increasing strain. This refers to a successive decrease of cluster size with strain due to stress-induced breakdown of filler clusters (see below). For prestrained samples, the cluster size remains unaltered, and the strain amplification factor X is constant, as far as the maximum prestrain is not exceeded, i.e., $X = X_{max}$.

In the case of fractal clusters, the value of the strain amplification factor X can be related to the structure of the filler clusters:[16]

$$X = 1 + \text{const}\left(\frac{\xi}{a}\right)^{d_w - d_f} \phi_F^{\,2/(3-d_f)} \quad (8)$$

Here, ϕ_F is filler concentration, a is filler particle size, ξ is cluster size, d_f is the fractal dimension, and d_w is the anomalous diffusion exponent of filler clusters. This constitutes a relation between X and the structure of the filler clusters as well as the filler concentration. In the case of percolation clusters as well as kinetically aggregated clusters it holds $d_w - d_f \approx 1.3$.[17] Since the exponent $d_w - d_f$ is in general positive, the strain amplification factor is a strictly monotone increasing function of the cluster size.

Straining of a virgin sample will result in a continuously decreasing strain amplification factor (stress softening), which corresponds to a successively decreasing cluster size. An empirical approach of this process has first been considered in ref 6. A constitutive generalization of the described procedure can be obtained by an averaging procedure over all space directions that leads to the scalar strain variable E:[18]

$$E := \sqrt{\frac{I_1}{3}} - 1 \quad \text{with } I_1 = \sum_{\mu=1}^{3}(1 + \epsilon_\mu)^2 \quad (9)$$

Two approaches for a constitutive inclusion of successive filler cluster breakdown are considered: cluster decay according to a power law and cluster decay according to an exponential law. In the first power law case it holds

$$\frac{\xi(E)}{a} = \left(\frac{\xi_0}{a} - 1\right)(1 + E)^{-\beta} + 1 \quad (10)$$

This yields the following strain amplification factor:

$$X(E) = X_{inf} + (X_0 - X_{inf})(1 + E)^{-y} \quad (11)$$

with the abbreviations $y = \beta(d_w - d_f)$. The quantities X_0 and X_{inf} denote the limiting strain amplification factors related to zero and infinite strain, respectively. They correspond to the initial cluster size ξ_0 and the final size $\xi = a$, where all clusters are broken:

$$X_0 = 1 + \text{const}\cdot\left(\frac{\xi_0}{a}\right)^{d_w - d_f}\phi^{2/(3-d_f)}; \quad X_{inf} = 1 + \text{const}\cdot\phi^{2/(3-d_f)} \quad (12)$$

As a second possibility, the cluster decay is assumed to follow an exponential law:

$$\frac{\xi(E)}{a} = \left(\frac{\xi_0}{a} - 1\right)e^{-\gamma E} + 1 \quad (10')$$

With the abbreviation $\alpha = \gamma\,(d_w - d_f)$ the corresponding strain amplification factor reads

$$X(E) = X_{inf} + (X_0 - X_{inf})e^{-\alpha E} \quad (11')$$

Below, we will apply these two empirical concepts to the analyses of uniaxial stress−strain data obtained for a variety of filler reinforced elastomer systems.

The rubber specific parameters G_c, G_e, and n_e/T_e can be estimated by fitting uniaxial stress−strain data of filled rubbers at various prestrains ϵ_{max} to eqs 6 and 7 with variable strain amplification factors $X = X_{max}$. From the obtained values of the cross-link modulus G_c the mechanically effective network chain density ν_{mech} (number per units volume of rubber matrix) can be evaluated by the relation

$$G_c = (1 - \phi_F)A_c\nu_{mech}RT \quad (13)$$

Here, $A_c \approx 0.67$ is a microstructure factor that considers the fluctuation of network junctions, i.e., cross-links and trapped entanglements,[5] ϕ_F is the filler volume fraction, R is the gas constant, and T is temperature.

The mechanically effective chain density ν_{mech} of filler reinforced rubbers can be assumed to consist of two parts: the chain density associated with polymer network junctions (cross-links and trapped entanglements) and the additional chain density ν resulting from polymer−filler couplings.[19] The first part scales with the volume fraction of the polymer matrix $(1 - \phi_F)$ and can be represented by the number of network chains per unit volume of the rubber matrix, ν_0; the second one varies linear with the filler volume fraction ϕ_F and the number of active sites per unit volume of fillers, ν_F. Then, by assuming a microstructure factor of polymer−

filler junctions to be equal to one (no fluctuations), one obtains

$$\nu_{\mathrm{mech}} = \nu_0 + \frac{\nu_{\mathrm{F}}\phi_{\mathrm{F}}}{A_{\mathrm{c}}(1-\phi_{\mathrm{F}})} \tag{14}$$

The two quantities ν_0 and ν_{F} can be evaluated from the dependency of the mechanically effective chain density ν_{mech} on filler volume fraction ϕ_{F}.

Experimental Section

Sample Preparation. All samples were prepared with a solution styrene butadiene rubber (SBR) often used in tire industry (BUNA VSL 2525-0) with 25 wt % styrene and 25 wt % vinyl units. The statistical and weight-averaged molar masses are 98 and 207 kg/mol, respectively. Fillers used were carbon black (N220) and silica (Ultrasil 7000 GR) with a silane coupling agent (Si 69).

Here unfilled styrene−butadiene rubber is simply designated as "SBR", while carbon black- or silica-filled samples are named using "C" or "S", respectively, followed by a two-digit number characterizing the filler weight fraction per 100 g of rubber (phr). For each filler type three composites were prepared to study the effect of filler concentration (40, 60, and 80 phr). Accordingly, the signature C40, C60, C80 is used for the samples filled with carbon black and S40, S60, S80 for those with silica.

Further two composites were prepared to investigate the effect of the polymer on filler networking: first, a composite with a reduced amount of cross-linking agent; second, a silica composite without coupling agent silane. Accordingly, the sample C60h contains half of sulfur and CBS in comparison to C60, and S60x is mixed like the sample S60, but without silane. In view of a reasonable filler dispersion and vulcanization behavior, all samples were compounded with 1 phr of stearinic acid and 2.5 phr of ZnO. Furthermore, 2 phr of IPPD and 1.5 phr of TMQ were added to all samples as aging protector.

For comparison reasons, cross-linked and un-cross-linked samples were prepared. The notation of un-cross-linked samples begins with an additional letter "U", e.g., USBR, UC60, and US60. The NMR response of the un-cross-linked and unfilled sample, USBR, was used as a measure of q_0, which involves the contribution of chain entanglements, both temporary and trapped.

The samples were prepared in an internal mixer (Werner & Pfleiderer GK 1.5 E) with a mixing chamber of 1500 ml and 6.5 min mixing time. For the silica/silane systems a two-step mixing procedure was applied. The vulcanization system, consisting of 2.5 phr of *N*-cyclohexylbenzothiazol-2-sulfenimide (CBS) and 1.7 phr of sulfur, was added separately on a roller mill. Cross-linked test samples were obtained by curing the composites at 160 °C up to the rheometer optimum.

NMR Measurements. All the SBR samples were measured on a Varian INOVA-400 spectrometer operating at a proton resonance frequency of 400 MHz. Their ^{1}H transverse magnetization decays were detected using the Hahn spin echo technique on a wide-line probe. Before each measurement, a 90° pulse length was accurately calibrated (2−3 μs) and tuned because the shape of magnetization decay curve was found to be very sensitive to exact tuning. Phase cycling was used, giving only negligible differences to a sequence with equal phases for both pulses. All the samples were measured after equilibrium at 80 °C (well above T_{g} + 120 K, with $T_{\mathrm{g}} \approx -47$ °C for SBR). The maximum intensity of the echo trace was fitted to eq 1 by nonlinear regression analysis using Microcal Origin 6.0 procedures (and compared with a home-built fitting program "xfit") and giving regression coefficients better than 0.98, mostly than 0.99. Also, proton $T_{1\rho}$ (the transverse relaxation time in the rotating frame) of all these samples were measured at the spinning frequency of 4 kHz and 40 °C, using a 7 mm MAS probe.

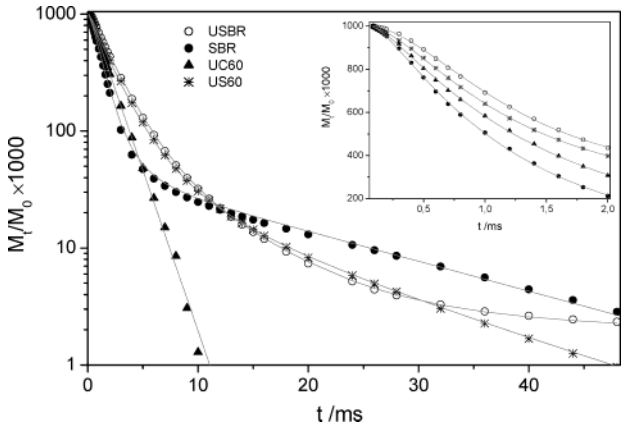

Figure 1. Transverse relaxation data (symbols) of un-cross-linked and cross-linked SBR samples from Hahn echo measurements at 80 °C. Solid curves denote the fitted results according to eq 1. The inset is the enlarged part at short echo times. The strongest differences can be seen at very short and very long times.

At this point a remark must be done concerning the certainty of the NMR results. The reproducibility of the results including the errors in the fitting procedure is better than 10%. However, the theoretic model for the determination of the molar mass M_{c} between two junction points depends on some assumptions (estimation of the *k*-factor, above-mentioned assumptions for the separation of different kinds of junctions, the applicability of the model used). Therefore, the total error was estimated on the order of 20%.

Mechanical Measurements. Uniaxial stress−strain measurements were performed on (S2) strip samples with a tensile tester (Zwick 1445). With 10 mm/min, a relatively low extension rate (of the cross head) was selected in all cases to minimize the dynamic contributions to stress. It corresponds to a strain rate of $\partial\epsilon/\partial t \approx 4 \times 10^{-3}\ \mathrm{s}^{-1}$. Two different kinds of experiments were performed: (i) discontinuous damage and (ii) continuous damage until rupture. In the case of discontinuous damage the sample is prestrained up to 100% three times. Then the strain is enlarged by an amount of 50%, and the whole procedure starts again. This successive increase of prestrain is carried out until rupture of the sample. The extensional phase of each third cycle is taken for a fit of the data points to the model. Between the individual measuring cycles, the specimens were allowed to relax for a period of 1 min. Continuous damage means that a virgin sample is strained without stop over up to rupture. For the whole set of data studied, the data points are shifted parallel to the strain axis so that all curves come from the origin of the coordinate system. This procedure eliminates the permanent set of the samples that is not considered in the model.

Results and Discussion

Analysis of NMR Data. Here, we will first focus on the NMR results that are compared to the mechanical analysis afterward. SBR samples filled with carbon-black (N220) and silica−silane were measured using the Hahn echo technique. An exemplary fit is shown in Figure 1. For comparison, USBR and SBR are also included in the figure.

The effects of vulcanization and filling are qualitatively clear and can be further quantified. According to eqs 1−3, we estimated the contents of different chain components and their mobility as well as M_{c} of network chains for SBR samples, both cross-linked and un-cross-linked, as listed in Tables 1 and 2. Furthermore, the dependence of main parameters on the content of fillers is shown in Figure 2. The comparison of the relative fraction of dangling ends $B = 1 - A - C$ with the theoretical value $2M_{\mathrm{c}}^{\mathrm{tot}}/M_{\mathrm{n}}$ gives a good agreement for

Table 1. Parameters of Network Structure of Un-Cross-Linked SBR According to Eqs 1−3[a,b]

sample	10^4q	M_c^{cor}, kg/mol	M_c^{tot}, kg/mol	$2M_c^{tot}/M_n$, %	τ_s, ms	τ_f, ns	τ_f^s, ns	A, %	B, %	C, %	const, %	$T_{1\rho}$, ms
USBR	0.895		6.2	12.7	0.30	16.0	0.38	88.5	11.2	0.3	0.05	7.3
UC60	1.88	13.8	4.3	8.8	0.19	33.6		96.1	3.9			5.6
US60	2.37	9.9	3.8	7.8	0.14	24.6	6.33	84.4	12.3	3.3	0.08	7.0

[a] For these un-cross-linked samples in comparison to Table 2 the values for G_c and G_e are missing because stress−strain measurements for such samples are not meaningful. [b] Note: here $T_{1\rho}$ analyses are also included. τ_f^s denotes the correlation time for the motion of free chains, obtained from T_{2s} values according to eq 2.

Table 2. Parameters of Network Structure of Cross-Linked SBR (First Nine Parameters According to Eqs 1−3)

sample	10^4q	M_c^{cor}, kg/mol	M_c^{tot}, kg/mol	$2M_c^{tot}/M_n$, %	τ_s, ms	τ_f, ns	τ_f^s, ns	A, %	B, %	C, %	const, %	$T_{1\rho}$, ms	G_c, MPa	G_e, MPa	n_e/T_e
SBR	1.52	20.4	4.8	9.7	0.53	43.6	1.03	86.4	9.8	3.8	0.01	4.4			
C40	1.82	14.6	4.4	8.9	0.37	34.8		94.8	5.2	0	0	4.5	0.182	0.713	100
C60	2.75	8.3	3.6	7.3	0.23	32.5		97.8	2.2	0	0	4.7	0.203	0.841	100
C80	4.32	5.2	2.8	5.8	0.16	25.9		99.2	0.8	0	0	4.8	0.246	0.989	100
C60h	2.41	9.7	3.8	7.8	0.21	25.2		98.9	1.1	0	0		0.085	0.481	165
S40	2.93	7.7	3.4	7.0	0.22	28.0	0.74	88.9	8.4	2.7	0.1	4.9	0.152	0.572	100
S60	3.05	7.4	3.4	6.9	0.19	26.6	6.71	89.7	6.8	3.5	0.1	5.3	0.145	0.610	100
S60[a]	3.04	7.4		6.9	0.19	21.1	4.91	87.0	9.3	3.7	0.1				
S80	6.78	3.6	2.3	4.6	0.09	24.6	9.15	90.1	5.0	4.9	0.1	5.2	0.196	0.667	100
S80[a]	6.12	3.9		4.9	0.09	24.9	7.37	86.0	8.7	5.3	0.08				
S60x	2.33	10.2	3.9	7.9	0.23	31.5	8.50	85.2	12	2.7	0.08		0.094	0.528	202

[a] Experimental results at 100 °C; see also note to Table 1.

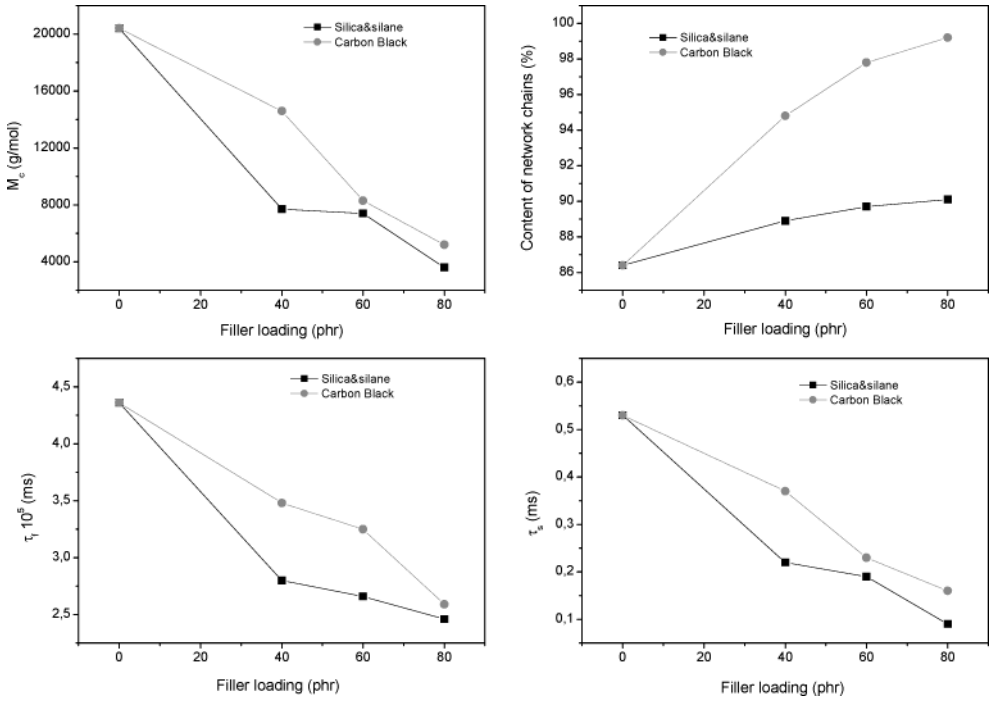

Figure 2. Plots of M_c, A, τ_f, and τ_s vs filler loading for the cross-linked SBR system. Solid circles denote samples filled with carbon black N220, and solid squares denote ones filled with silica−silane. The content of cross-linker is the same for all samples.

the unfilled samples USBR and SBR as well as for the silica filled ones. For carbon black filler, however, the values found from NMR are much smaller. This supports our finding (see below) that N220 has a stronger adsorptivity and fixes the originally free dangling ends. It can be seen directly from the experiment result in Figure 1, where a long tail, characteristic for the dangling chain ends, can be observed for the silica-filled samples only. That means this result is valid independently on the special model used.

First, it can be clearly seen from Table 2 and Figure 2 that for cross-linked SBR elastomers q significantly increases with increasing of filler loading, especially for silica-filled SBR (S40, S60, and S80), indicating the decrease of molecular mass, M_c, between cross-linking points or the increase of cross-linking density due to the inclusion of fillers. At the same time, the relative content of cross-linked chains significantly increases with increasing of filler loading, especially for N220-filled SBR (C40, C60, and C80). Accordingly, the relative content of dangling chain ends, which originate from chain ends of the precursor, decreases. This shows that chain ends of a precursor are increasingly bound to the filler surface due to further increase of fillers and become part of network chains. Therefore, filler particles behave like additional cross-linking points, partly due to their chemical binding with polymer chains and partly due to their surface adsorption. Comparing SBR samples filled with N220 and silica−silane, one observes that at the same loading N220 always yields higher

content of network chains but also higher value of M_c (see Figure 2). Similar results are obtained for un-cross−linked SBR elastomers (USBR, US60, and UC60).

Also, it is clear from Tables 1 and 2 that for SBR filled with silica−silane, free silane further contributes to the tail of transverse magnetization decay, leading to the additional increase of "sol" fraction with increasing fillers silica−silane. Evidently, a part of "sol" indeed comes from free chains in the network matrix, as revealed by S60x, i.e., SBR filled with silica only. Conversely, for SBR filled with N220, no "sol" fraction can be observed. Hence, this further demonstrates the fact that N220 really possesses the stronger adsorption or binding ability. In the presence of carbon black N220, free chains, just because of their free motion, are completely adsorbed at the surface of N220 aggregates, concomitant with only few additional dangling chains.

The influence of filler on the molecular mobility is complicated and different for both un-cross-linked and cross-linked SBR systems. Let us first consider cross-linked SBR. From Table 2 or Figure 2 it can be seen that the correlation time of chain segments τ_f decreases with the introduction of fillers N220 or silica−silane and further decreases (from 40 to 80 phr). Accordingly, in the presence of fillers, local segmental motion is accelerated. At the same time, τ_s decreases with increasing of filler loading, reflecting the faster overall motion of molecular chains. This tendency is more apparent for silica−silane-filled systems. The above results (achieved from Hahn echo measurements) are further supported by proton $T_{1\rho}$ measurements. Two relaxation components were always observed for each of the samples and can give better fitting than a single component. But the difference of both components was found to be indeed small, and thus their weighted average $T_{1\rho}$ values, which can be otherwise obtained by one−component analysis, were calculated and listed in the last column of Tables 1 and 2. Obviously, the decay time constant $T_{1\rho}$ increases with the introduction and raise of the content of silica−silane. Variable-temperature measurement shows the higher $T_{1\rho}$ is, the faster molecular motion. Hence, it is clear that molecular motion becomes faster due to the introduction and further increase of silica−silane. SBR samples filled with N220 show the same (but small) tendency. Anyway, the indications from the transversal relaxation (τ_s, τ_f) as well as from $T_{1\rho}$ measurements show that the mobility at least will be not decreased under the influence of the filler. The possible explanation is as follows: In the presence of fillers, the chemical cross-linking reaction in the rubber matrix is restrained to some extent, as proposed by Mark et al.[20] Probably, a part of the curatives is adsorbed at the filler surface, which reduces the cross-linking efficiency. In other words, the contribution from chemical cross-linking of the polymer matrix reduces as the filler content increases, though the same amount of curatives has been applied per unit mass of polymer. This is in line with the observation that τ_f as well as τ_s decreases from C60 to C60h, where half of the amount of curatives is used.

At the same time, probably because polymer−filler junctions do not so effectively restrain segmental and molecular motion as chemical cross-linking points caused by cross-linkers, the phenomenological dynamic behavior of two kinds of network chains of different origins is, on average, accelerated rather than attenuated. It should be noticed that Hahn echo measurements cannot differ between constraints by physical and chemical junctions. (For this reason the q_0 correction, above-described, was introduced.) Compared with N220-filled SBR, the faster motion (longer T_2 values and shorter τ_s) of silica-filled SBR possibly demonstrates that chemical cross-linking reaction is restrained to a greater extent in the presence of silica−silane. Motional constraint exerted by the filler is poorer than that by chemical cross-linking points in a matrix, but the former can be still clearly observed for the "sol" fraction of silica−silane-filled SBR. As compared with SBR (cross-linked, unfilled), the T_{2s} value of silica−silane-filled SBR apparently decreases, revealing less mobility experienced by "sol" fraction, including free chains. In fact, motional constraint may occur through adsorption−desorption equilibrium of free chains and silane. Furthermore, the T_{2s} values of silica−silane-filled samples further decrease with the increase of fillers, indicating that the residence time of free chains and silane on the surface of fillers increases with the increase of surrounding filler particles.

Conversely, in the absence of chemical cross-links, the effect of filler is only to act as cross-linking points, and so the molecular motion is expected to become slower for the un-cross-linked SBR system. The substantial increase in τ_f from 16 to about 30 ns (see Table 1) just shows the constraint of segmental motion exerted by fillers, although overall chain motion, as revealed by the decrease in τ_s from 0.3 to ∼0.15 ms, is slightly faster. Proton $T_{1\rho}$ measurements also confirm the attenuation of segmental or chain motion. Obviously, the proton $T_{1\rho}$ values (see Table 1) of a SBR decrease due to the introduction of fillers. Hence, molecular motion becomes slower due to the introduction of fillers. Furthermore, we observed that for SBR filled with N220 molecular mobility is lowered to a greater extent.

The effect of chemical cross-linking is examined by comparing the NMR data in Tables 1 and 2. Through the comparison of un-cross-linked and cross-linked SBR, e.g., UC60 and C60, both of which are filled with 60 phr of N220, it can be clearly seen that subsequent vulcanization definitely leads to a slower mobility and an increase of the amount A of network chains, concomitant with the increase of cross-link density. The same is true for SBR filled with 60 phr of silica−silane. The comparison between C60h and C60 or between USBR and SBR also emphasizes that cross-link density increases, and at the same time, segmental/overall chain motions decrease with the increase of cross-linking agent. The above results are in good agreement with previous studies on the specific effect of cross-linker on unfilled rubbers.[1−3]

The addition of silane does not lead to substantial variation of structural and dynamic parameters, except for the increase of the amount A of inter-cross-link chains and sol fraction C. As mentioned above, the increase of sol fraction is mainly due to the contribution of silane itself. On the other hand, close inspection of the echo signals at very short decay times reveals the existence of an additional fast-decaying Gaussian component with a second moment of ∼600 ms^{-2}. Its content increases due to the addition of silane or subsequent cross-linking, as shown in Figure 3. Obviously, it can be assigned to the contribution of bound rubber since very strong dipolar coupling still exist for its neighboring protons. Of course, the contributions from tightly adsorbed units among bound rubber and occluded

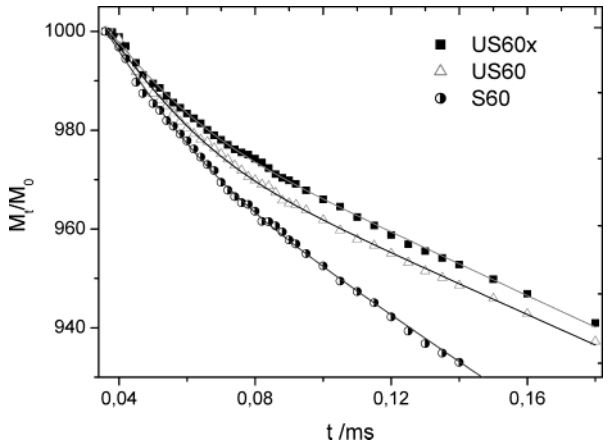

Figure 3. Observation of an fast-decaying component at very short echo time (additional to the exponential component with much higher intensity) from Hahn echo measurements at 80 °C. A Gaussian function fits well this relaxation part, yielding its amount from 4%, 4.6%, to 5.2% for US60x, US60, and S60, respectively, with a second moment of ~600 ms^{-2}.

rubber may be lost due to the limitation of instrumental dead time and the disturbance of background signal. Anyway, it is certain that the main effect of silane is to facilitate the formation of the bound rubber through its chemical linkage with the filler surface. This will in turn influence the deformation behavior of a rubber matrix. Here it must be noted that this Gaussian component is not included in the previous Hahn echo observations and fitting procedures because it arises from the immobilized part of SBR chains, but not network chains themselves. Similar observations of bound rubber were also obtained for N220-filled SBR. The dependence of bound rubber on the type and content of fillers will be reported in a separate paper.

The effect of rising temperature above 80 °C, e.g. at 100 °C, is mainly an acceleration of molecular motion, as expected. Furthermore, dangling chains remarkably increase and, at the same time, free chains slightly increase. This can be attributed to the desorption of some chains or segments. Despite these variations, q is almost constant and thus characteristic of this elastomer system at temperature well above T_g + 120 K.

Mechanical Analysis. Exemplary stress−strain results of the sample with 60 phr of carbon black and corresponding fits are shown in Figure 4. The fitting parameters are inserted in the legend. Obviously, the prediction of the model is in good agreement with experimental data. In particular, the data of prestrained samples are well described by eqs 6 and 7 with constant strain amplification factor X_{max} for every prestrain ϵ_{max}. Thereby, a single set of polymer parameters G_c, G_e, and n_e/T_e is used for all prestrains. The stress−strain data of the virgin sample are fitted with the same set of polymer parameters by using eqs 6 and 7, but with a strain-dependent amplification factor according to eqs 11 or 11′, respectively. It becomes clear that both empirical cluster decay laws can be applied for a description of the stress−strain behavior during the first stretching cycle of the virgin sample, though the power law decay eq 11 gives a better fit to experimental data at very large strains (dashed line in Figure 4).

As shown in the legend of Figure 4, the obtained amplification factors X_{max} of prestrained samples decrease successively with increasing prestrain ϵ_{max}. This behavior is shown to be fulfilled for all filled SBR

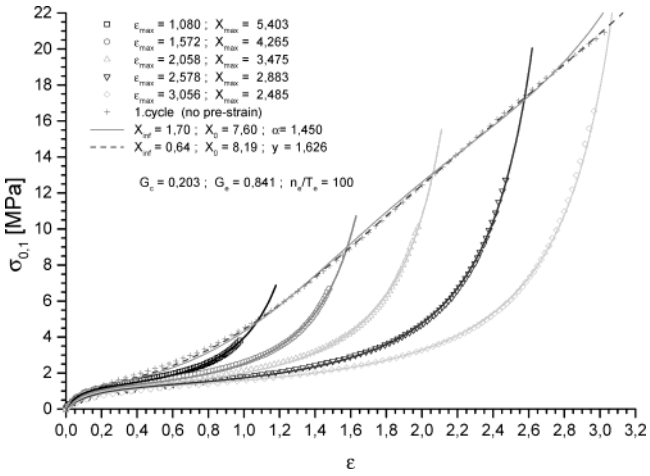

Figure 4. Uniaxial stress−strain data (symbols) and fitting curves (lines) of the SBR sample with 60 phr of N220 (C60). The first stretching of a virgin sample (upper curve) and the third stretching of preconditioned samples at various prestrains (lower curves) are presented. Fitting parameters are shown in the legend.

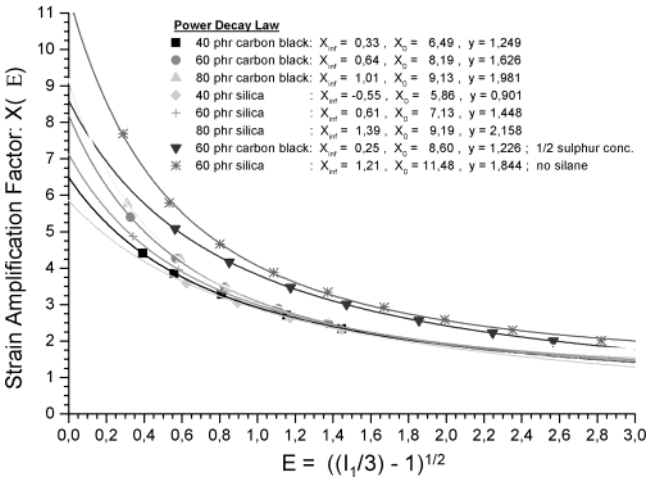

Figure 5. Estimated strain amplification factors X_{max} at different prestrains (symbols) vs strain variable E for the filled samples at various prestrains. The solid lines are fitted according to the power law of cluster decay eq 11 with fitting parameters as shown in the legend.

samples in Figure 5, where the obtained amplification factors X_{max} are plotted against the strain variable $E(\epsilon_{max})$ (symbols). The fitted lines in Figure 5 demonstrate that the dependency of X_{max} on prestrain can be well described by the power law eq 11. The obtained exponents and limiting amplification factors X_0 and X_{inf} are listed in the legend of Figure 5. They describe the variation of the amplification factor during the first extension of the virgin samples, which is used for the simulation of stress−strain curves in Figure 4 (dashed line). Obviously, the amplification factors X_0 and X_{inf} increase with filler concentration, but also the exponent y increases, implying that the stress-induced breakdown of filler clusters is not universal. Furthermore, the amplification factors of the carbon black-filled systems are found to be somewhat larger than the corresponding silica−silane systems at the same level of loading. This indicates that the cluster size is larger in the case of carbon black, implying a higher stability of filler−filler bonds in the carbon black clusters. The largest amplification factors are found for the silica-filled sample without coupling agent silane (S60x) and the carbon

Table 3. List of Fitting Parameters and Evaluated Network Chain Density ν_{mech} from Stress−Strain Data and ν_{NMR} from NMR Data, Respectively, for Variously Filled SBR Samples (ν^*_{NMR}: without q_0 Correction) and Separation of Several Contributions to the Network Density

sample	ϕ_F	ν_{mech}	ν_0	ν_F	b_{PF}, nm	ν_{NMR}	ν^*_{NMR}	$\nu_{mech} - \nu_{NMR}$	$\nu^*_{NMR} - \nu_{mech}$	$\nu^*_{NMR} - \nu_{NMR}$
USBR	0						128			
UC60	0.231					63	201			138
US60	0.213					76	198			122
SBR	0					38	163			125
C40	0.167	131	52	251	1.2	58	195	64	64	137
C60	0.231	158	52	251	1.2	106	247	38	89	141
C80	0.286	206	52	251	1.2	171	314	19	108	143
C60h	0.231	65				92	234		169	142
S40	0.153	107	46	197	1.7	104	232		125	128
S60	0.213	110	46	197	1.7	110	239		129	129
S80	0.265	160	46	197	1.7	228	358		198	130
S60x	0.213	72				75	198		126	123
junction type										
cross-links[a]		√	√			√	√			
network−filler links		√		√		√	√			
trapped entangl.		√	√				√	√		√
tempor. entangl.							√		√	√

[a] For cross-linked SBR systems only.

black-filled sample with half amount of cross-linking agent sulfur (C60h). Obviously, the cluster size for these two systems reaches a maximum because on the one side, pure silica fillers form very stable clusters due to strong dipolar interaction. On the other side, the cluster size in the weakly cross-linked system C60h is relatively large because the stress on the clusters, which is transmitted by the rubber matrix, remains smaller.

A list of the adapted polymer parameters for all sample types is given in Table 2. The cross-linking modulus G_c as well as the topological constraint modulus G_e is found to increase with filler concentration for both filler types. This tendency is just parallel with the decrease in the NMR-derived M_c and the increase in network chains. It is clear that the first effect of G_c results from the successive increase of polymer−filler couplings that act as additional junctions. The latter has been revealed on a molecular level by the above Hahn echo measurements. The observed effect of filler concentration on G_e refers to the reinforcing influences of filler clusters.[21] As compared with the samples filled with silica−silane, the higher G_c values were always obtained for the N220-filled samples that, however, possess higher NMR-derived M_c values. One tentative interpretation is that chain entanglements may be significantly trapped in N220-filled samples due to the stronger physical adsorption of chains on N220 and thus contribute to the estimation of G_c. Note that, apart from the samples C60h and S60x, the value $n_e/T_e = 100$ has been prechosen due to technical reasons and is not fitted (compare ref 6). The chosen fixed value allows for a reasonable fit of stress−strain data, independent of filler type and loading. A variation of the finite extensibility parameter n_e/T_e has a small effect on G_c and G_e, only but mainly alters the level of the strain amplification factors. For that reason the samples C60h and S60x show the largest strain amplification factors in Figure 5. However, even with a freely fitted finite extensibility parameter n_e/T_e, the adaptations of stress−strain cycles for the samples C60h and S60x were poor, indicating that the mechanically obtained parameters for these systems are not very save. The samples C60h and S60x show significantly lower moduli, which can be attributed to lower cross-link densities and higher M_c values, compared to those of C60 and S60, as revealed by the Hahn echo technique.

The data obtained with eq 13 for the mechanically effective chain density ν_{mech} are listed in Table 3. Obviously, ν_{mech} increases significantly with filler concentration and is generally larger for the carbon black-filled systems as compared to the silica−silane systems. This difference between the two types of fillers can be traced back to a different coupling density between polymer chains and filler surface if the decomposition of ν_{mech} according to eq 14 is applied. From the averaged variation of ν_{mech} with filler concentration one obtains the following values for the chain density ν_0 of the rubber matrix and the chain density ν_F due to polymer filler couplings: $\nu_0 = 52$ μmol/cm^3, $\nu_F = 251$ μmol/cm^3 in the case of carbon black and $\nu_0 = 46$ μmol/cm^3, $\nu_F = 197$ μmol/cm^3 in the case of silica−silane. This confirms that the cross-link density of the rubber matrix is slightly larger for the carbon black-filled samples, as concluded from the NMR result of a lower segmental mobility in these systems (larger correlation time τ_f). Note however that in deriving eq 14 the cross-linking density of the polymer matrix is assumed to be independent of filler concentration. This seems not to be fulfilled strictly in view of the observed acceleration of fast segmental motion τ_f with increasing filler loading, as discussed above in the context of Table 1. Nevertheless, the obtained values of ν_F allow for a rough estimation of the mean distance b_{PF} of polymer chains bonded to the filler surface if the specific surface area S_F of the two filler types is considered together with the simple scaling relation $b_{PF}^2 \approx S_F\rho_F/(\nu_F N_A)$ (N_A = Avogadro's constant). With $S_F = 116$ m^2/g and $\rho = 1.85$ g/cm^3 for N220 one obtains $b_{PF} \approx 1.2$ nm for the carbon black systems, while $S_F = 175$ m^2/g and $\rho = 2.0$ g/cm^3 for Ultrasil 7000 GR yields $b_{PF} \approx 1.7$ nm for the silica systems. Both values appear reasonable since they are within the same order of magnitude as the statistical segment length of the chains. They demonstrate that the mean distance between adjacent polymer filler couplings is generally larger in the silica systems. The coupling parameters ν_F and b_{PF} agree fairly well with mechanical and transversal NMR relaxation data found in the literature for carbon black-filled elastomers.[19,22]

A rough estimation of the number of chain densities associated with polymer/filler junctions is possible using the NMR data, too. According to the remarks below eq 4, these values can be calculated from the differences

in the total concentration of network junctions for UC60 and USBR or for C60 and SBR, giving the values 73.5 or 84.5 μmol/cm^3, respectively, in relation to the rubber volume. The average of both values related to the filler volume gives an averaged result $\nu_F = 263\ \mu$mol/cm^3, very close to the value found by the mechanical measurements discussed above. For silica-filled rubber, however, the corresponding values are 70.4 and 76.2 μmol/cm^3, respectively, and $\nu_F = 271\ \mu$mol/cm^3 is much larger than that found by modulus measurements. The reason for this deviation could be that the number of chemical cross-links for unfilled and filled rubbers is not constant.

As already mentioned, this separation can be done under the assumption of a constant number of cross-links and entanglements independently of the filler content (and it was performed for the samples with 60 phr of filler because we had only un-cross-linked samples for this filler content). But, we do not think that this assumption is generally correct because the number of chemical cross-links is influenced by the presence of filler during the vulcanization process. Therefore, we did not try a determination of ν_0 and ν_F like for the mechanical measurements, although (especially for carbon black filler) a good linear behavior according to eq 14 can be observed. However, there are strong deviations of the linearity if one includes the unfilled sample.

The values of the mechanically effective chain density ν_{mech} agree fairly well with the ν_{NMR} data, though significantly higher values of ν_{mech} are found for the carbon black-filled systems, which were calculated according to eq 4. Usually, ν_{mech} is composed of the contributions from cross-link points, trapped entanglements, and network links on the filler, whereas, the ν^*_{NMR} includes the contributions from cross-link points, network links on the filler, and permanent and temporary entanglements. After q_0 correction, the ν_{NMR} only includes the first two contributions; in other words, the contribution of all the chain entanglements, whether trapped or not, is excluded. Obviously, for silica−silane-filled samples the mechanically effective chain density well corresponds to the NMR-derived cross-link density, i.e., ν_{NMR} with q_0 correction (see column 7 in Table 3). This implies that most of chain entanglements are not trapped in silica−silane-filled SBR. However, for N220-filled samples, the ν_{mech} is relatively higher than ν_{NMR} with q_0 correction but still lower than the NMR-derived total cross-link density, i.e., ν_{NMR} without q_0 correction. This indicates that part of chain entanglements is trapped in N220-filled SBR. Another possibility is that bound rubber may contribute to mechanical measurements to greater extent for N220-filled samples, thus leading to their larger values of ν_{mech}. In contrast, the effect of bound rubber itself was not involved in the model concerning the calculation of ν_{NMR}.

The relations of the three different kinds of cross-link density (ν_{mech}, ν_{NMR}, and ν^*_{NMR}) were also demonstrated in Table 3. From their differences the densities for the trapped and the temporary entanglements are determined separately. Of course, one has to be careful in the interpretation of these data because differences of parameters from quite different methods are compared, where systematic errors cannot be excluded.

On the basis of the above NMR and mechanical analyses, we tentatively propose the schematic representation for the two types of filled systems shown in Figure 6. In terms of these schemes, the larger N220 aggregates are more inhomogeneously dispersed in a rubber matrix, and the distance between them is correspondingly larger, thus leading to bigger M_c*. On the other hand, because of their stronger binding ability, these aggregates can still attach more polymeric chains to their surfaces, thus leading to more inter-cross-link chains and partial trapping of chain entanglements. On the contrary, the filler silica, because of more homogeneous dispersion of smaller silica aggregates in the SBR matrix, can more effectively decrease M_c than N220. But their weaker binding ability or adsorbability makes that more polymeric chains survive as dangling and free chains. Here it is noticed that chemical cross-linking points shown in Figure 6a,b exist only for cross-linked SBR and that part of chains depicted within filler aggregates denotes occluded chains.

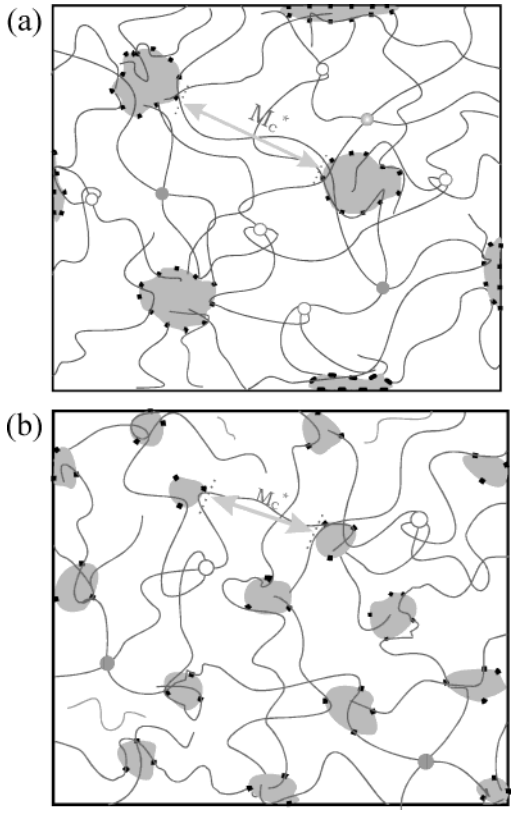

Figure 6. SBR systems filled with N220 **(a)** and silica−silane **(b)**. Filled and open circles denote the chemical cross-linking points and trapped entanglement points, respectively. Black dots represent the polymer−filler couplings due to active sites on the filler surface.

Conclusions

In summary, from the above measurements and analyses several main conclusions can be drawn:

1. The density of network junctions of filled SBR systems increases with increasing the content of fillers, as confirmed by both NMR and mechanical measurements.

2. A decomposition of network junctions in polymer−polymer and polymer−filler junctions could be performed, demonstrating that the main contribution comes in from the polymer filler couplings, which is significantly larger in the case of carbon black as compared to silica−silane. The evaluated mean distance of adjacent polymer−filler couplings equals 1.2 nm for N220 and 1.7 nm for silica−silane-filled systems.

3. The trapped entanglements are more significant for a N220-filled SBR system but less important for a silica−silane-filled SBR system.

4. For N220-filled SBR more additional polymer−filler junctions and therefore less free dangling ends or free chains occur because of the higher adsorbability, whereas in silica−silane-filled SBR the network density is higher caused by a higher dispersity of the filler.

5. From NMR measurements it can be additionally seen that for a N220-filled SBR system the amount of network chains is higher and their mobility is lower, as compared with a silica−silane-filled SBR system.

6. The filler dependence of segmental and overall chain mobility is definitely different for both filled SBR systems, subsequently cross-linked and un-cross-linked, which is attributed to the restriction of the filler on the chemical cross-linking reaction occurred in a SBR matrix, probably due to the adsorption of curatives at the filler surface.

Acknowledgment. The authors are indebted to Prof. R. H. Schuster and Dr. H. Menge for stimulating discussions, to Dr. J. Meier and Mrs. K. Nowak for the help in sample preparation, and to the DFG (SFB 418), DKG, Columbian Chemicals Co., and Continental AG for financial support.

References and Notes

(1) Klüppel, M.; Menge, H.; Schmidt, H.; Schneider, H.; Schuster, R. H. *Marcromolecules* **2001**, *34*, 8107.
(2) Menge, H.; Hotopf, S.; Heuert, U.; Schneider, H. *Polymer* **2000**, *41*, 3019.
(3) Heuert, U.; Knörgen, M.; Menge, H.; Scheler, G.; Schneider, H. *Polym. Bull.* **1996**, *37*, 489.
(4) Heinrich, G.; Straube, E.; Helmis, G. *Adv. Polym. Sci.* **1988**, *85*, 33.
(5) Klüppel, M.; Heinrich, G. *Macromolecules* **1994**, *27*, 3596.
(6) Klüppel, M.; Schramm, J. *Macromol. Theory Simul.* **2000**, *9*, 742.
(7) Fedotov, V. D.; Tshernov, V. M.; Khasanovitsh, N. *Vysokomol. Soedin. A* **1978**, *XX*, *4*, 919. The English version of this journal is entitled *Polym. Sci. USSR*.
(8) Simon, G.; Schneider, H.; Häusler, K.-G. *Prog. Colloid Polym. Sci.* **1988**, *78*, 30.
(9) Simon, G.; Birnstiel, A.; Schimmel, K.-H. *Polym. Bull. (Berlin)* **1989**, *21*, 235.
(10) Abragam, A. *The Principles of Nuclear Magnetism*; Oxford University Press: New York, 1961.
(11) Gotlib, Yu. Ya.; Lifshitz, M. I.; Shevelev, V. A.; Lishanskij, I. S.; Balanina, I. V. *Vysokomol. Soedin.* **1976**, *A28*, *10*, 2299.
(12) Fry, C. G.; Lind, A. C. *Macromolecules* **1988**, *21*, 1292. Simon, G.; Götschmann, B.; Matzen, D.; Schneider, H. *Polym. Bull. (Berlin)* **1989**, *21*, 475.
(13) Fetters, L. J.; Lohse, D. J.; Richter, D.; Witten, T. A.; Zirkel, A.; *Macromolecules* **1994**, *27*, 4639.
(14) Aharoni, S. *Macromolecules* **1986**, *16*, 1722; **1986**, *19*, 426.
(15) Edwards, F.; Vilgis, T. A. *Rep. Prog. Phys.* **1988**, *51*, 243; *Polymer* **1986**, *27*, 483.
(16) Huber, G.; Vilgis, T. A. *Kautschuk, Gummi, Kunststoffe* **1999**, *52*, 102.
(17) Klüppel, M.; Schuster, R. H.; Heinrich, G. *Rubber Chem. Technol.* **1997**, *70*, 243.
(18) Heinrich, G.; Klüppel, M.; Vilgis, T. A. *Curr. Opin. Solid State Mater. Sci.* **2002**, *6*, 195.
(19) Heinrich, G.; Vilgis, T. A. *Macromolecules* **1993**, *26*, 1109.
(20) Mark, J. E., et al. *Science and Technology of Rubber*, 2nd ed.; Academic Press: New York, 1994.
(21) Klüppel, M.; Meier, J. Modeling of Soft Matter Viscoelasticity for FE-Applications. In Besdo, D., Schuster, R. H., Ihlemann, J., Eds.; *Constitutive Models for Rubber II*; Balkema, A. A., Lisse, Abingdon, Exton, Tokyo, 2001; pp 11−19.
(22) Lüchow, H.; Breier, E.; Gronski, W. *Rubber Chem. Technol.* **1997**, *70*, 746.

MA035985U